1,2,3-Benzotriazole Derivatives Adsorption on Cu(111) Surface: A DFT Study

Mario Saavedra-Torres[1], Carlos A. Escobar[1], Fernanda Ocayo[1], Frederik Tielens[2,*], and Juan C. Santos[1,*]

[1]Laboratorio de Corrosión, Departamento de Ciencias Químicas, Facultad de Ciencias Exactas, Universidad Andres Bello, Av. República 275, Santiago, Chile.

[2]Sorbonne Universités, UPMC Univ Paris 06, CNRS, Collège de France, Laboratoire de Chimie de la Matière Condensée de Paris, 4 place Jussieu, 75252 Paris Cedex 05, France.

Abstract

In the context of copper corrosion passivation, the adsorption of benzotriazole (*BTAH*) and its derivatives: 5-Methyl, 5-Amine, 1-Amine, 1-Methyl on a Cu(111) surface was investigated using periodic density functional (DFT) calculations. The results were contrasted with experimental ASTM protocols. Adsorption of *BTAH* and radical (*BTA*●) forms, as well as solvent effect were evaluated. The Cu-N interaction provides stable complexes with adsorption over top sites. Radical forms yielded more stable complex. Their adsorption energies correlate with the substituent position and electronic features. And finally, a strong interaction was obtained when the charge transfer goes from surface to adsorbate.

Keywords: Corrosion; Copper; Benzotriazole; Dibenzyl Disulfide; DFT; Adsorption

*Corresponding authors:
Juan C. Santos: jsantos@unab.cl
Frederik Tielens: frederik.tielens@upmc.fr

Introduction

1,2,3-Benzotriazole (*BTAH*) is a compound of important industrial interest, commonly used as passivator to mitigate the corrosion on metals such as copper and its alloys[1-16]. BTAH adsorption over metal surfaces has been particularly effective to mitigate copper corrosion under conditions simulating those found in electrical power transformers, e.g. [7, 13, 17-21]. The origin of copper coils deterioration by corrosion has been attributed to sulfured species, particularly to both dibenzyl disulfide (*DBDS*) and benzyl sulfide (*BS*)[22-25]. These antioxidants are additives added to improve the tribological properties of the insulating mineral oils, present in the power devices[22, 26]. In the corrosion process, the formation of copper (I) sulfide, Cu_2S, and other organic secondary subproducts, such as dibenzyl sulfide and bibenzyl, have been described[22, 27-30].

Although, the passivator effect of *BTAH* has been described abundantly, aspects such as the adsorption nature over surface defects, the influence of the solvent, and the introduction of substituents in *BTAH* core acting as passivator, remain unclear.

Passivator molecules adsorb on a surface and interact through their functional groups as a function of temperature, concentration (pressure), and chemical environment. Small organic molecules adsorbed on metal surfaces are studied in order to understand the more fundamental chemical phenomena occurring at the surface/molecule interface.[31]

In the present paper, the nature of the interaction between copper surface, Cu(111), and some *BTAH* derivatives are theoretically studied and compared with the results obtained in experimental assays of copper corrosion/inhibition in dielectric oils, in line with our former studies[32-34]. Our results are compared with those previously reported for similar systems as well as with similar works, clarifying some unclear aspects related to copper passivation. In particular, the energetic and electronic properties have been studied at the DFT level. The study is oriented to characterize locally the copper-nitrogen interaction. Additionally, the effect of solvent was considered, evaluating its role over the passivation capacity of the adsorbate.

Experimental Details

Inhibition Performance

To test the corrosion capabilities of dielectric transformer oils, the (American Society of the international association for Testing and Materials) ASTM D1275 B and D130/IP154 methodologies were implemented. The procedure for evaluating these capabilities is described in the Standard Test Method for Corrosive Sulfur in electrical oils, ASTM D1275-06. Typically, corrosion assays were performed as follows: a L-shaped folded polished copper strip (5 cm long × 1.3 cm wide) was washed with acetone and dried at room temperature. It was submerged in the investigated dielectric transformer oil (250 mL) contained in a 250 mL Duran glass bottle. Then, to eliminate the dissolved air, the oil containing the copper strip was bubbled for 5 min with nitrogen, and rapidly sealed with a Duran screw cap GL45. Two replicates for each oil tested were prepared, and then, simultaneously exposed to 150º C for a period of 72 hours in an oven with temperature control. At the end of this time period, the flasks were allowed to cool down and then, the copper strips were removed from the oil, and its coloration compared with the D130 ASTM copper strip corrosion color scale, in order to assess the corrosion extent, produced by the oil components over the copper strip.

To assess the inhibition capabilities of a series of different benzotriazoles (See BTAH, 5-Methyl-BTAH, 5-Amine-BTAH in **Figure 1**), an inhibition assay was conducted following the procedure described previously in this section but using 250 mL of an oil solution containing 200 ppm of DBDS. Then, different amounts of the benzotriazole derivative to be tested were added in order to reach 2, 3 and 4 ppm benzotriazole/250 mL oil. The inhibition effectiveness was measured using the D130 ASTM copper strip corrosion color scale.

Computational Details

Computational Methods

Since some reports describing the adsorption of both BTAH and BTA● (their deprotonated radical form) on copper surfaces has been described previously[7, 21,35], in this work the adsorption

of both species has been considered and the results will be compared with those reported for DBDS (strong corrosive agent) adsorption on copper surface. The different benzotriazole derivatives studied in this work are shown in **Figure 1**.

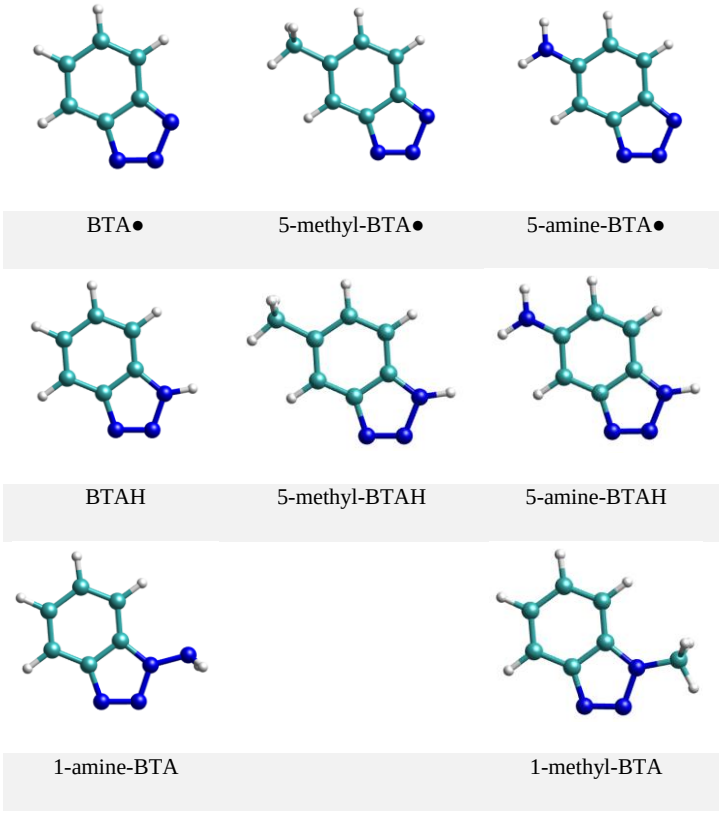

Figure 1. Structures of radical and molecular benzotriazole derivatives. In the ball-and-stick representation, carbon, nitrogen, and hydrogen atoms are colored in green, blue, and white, respectively.

All calculations were performed under the periodic DFT framework by means of the Vienna Ab Initio Simulation Package (VASP 5.3). The interactions represented by the valence electrons were described by the projector augmented wave (PAW) method with a cutoff of 400 eV. The Perdew-Burke-Ernzerhof (PBE)[36, 37], a Generalized Gradient Approximation (GGA) functional, were used.

The adsorption of benzotriazole molecules was modeled using a 4×4 unit cell of the Cu(111) surface. The molecules are at large enough distance from each other, in order to avoid

intermolecular interactions and/or SAM formation. The Cu slab was built considering 6 layers. Three bottom layers were kept fixed. Several DFT methods were tested, considering dispersive interaction corrections. The sampling in the Brillouin zone was performed employing 13 and 25 k-points, resolved on 5×5×1 and 7×7×1 grids for the geometry optimizations and energy evaluation (at PBE level), respectively. A vacuum space distance of 10 Å was considered, measured from the top of the adsorbated molecule to the image surface bottom layer.

The geometry optimization procedure consisted in locating initially the adsorbates at 2.5 Å from the surface, at the start of the relaxation. This distance was taken from chemi- and physisorption data reported in several previous studies involving the adsorption of sulfur molecules on copper surfaces[38-41].

Lattice Parameters

To evaluate the lattice parameters, a set of DFT methods, including van der Waals (vdW) interaction corrections were considered. They were obtained from a cell volume optimization of the FCC Cu primitive cell.

The lattice parameters obtained under selection of DFT methods were PBE-D2 (3.57 Å), PBE-TS (3.55 Å), PBE (3.63 Å) and compared with experimental one [42] (3.61 Å). Dispersion corrections Grimme D2[43] and Tkatchenko-Scheffler, (TS)[44], were evaluated for comparative reasons. It shows that the PBE method (without dispersion), provides a good approximation to the experimental data.

Adsorption energy and charge transfer calculations

Each complex can be characterized by its adsorption energy, ΔE_{ads}, which was calculated from the total energy of the ground state optimized geometries for the complex Cu(111)-BTA and clean Cu(111) slab and *BTA• (or BTAH)*, as follows:

$$\Delta E_{ads} = E_{Cu(111)\text{-}BTA} - [\, E_{Cu(111)} + E_{(BTA\bullet,\ or\ BTAH)} \,] \quad (1)$$

Moreover, an energetic decomposition scheme of deformation/interaction[45] can be included, to describe energetically the change along the adsorption process. This energetic partition scheme, as also used previously in our studies[32, 33], consists of energetic contributions of deformation (ΔE_{def}) and interaction (ΔE_{int}), related as:

$$\Delta E_{ads} = \Delta E_{def} + \Delta E_{int} \quad (2)$$

where $$\Delta E_{def}(X) = E(X_{deformed}) - E(X_{equilibrium,\ isolated}) \quad (3)$$

With X = $Cu_{(111)}$ *BTA•* or *BTAH*. The first term in the right-hand side of equation 2 represents the molecular geometry deformation from their equilibrium structure to the geometry acquired in the adsorption complex, and the second one, the interaction between those distorted structures.

The amount of total electronic charge transferred between adsorbent and the Cu surface, was quantified by a Global Charge Transfer descriptor (*GCT*), which corresponds to the sum of atomic charges (q_A) on each molecule (A), i.e. the *BTA* or the surface:

$$GCT = \sum_A q_A \quad ; \quad A \in BTA\bullet(or\ BTAH), Cu \quad (4)$$

For this purpose the Bader Charge Analysis[46, 47] was used.

The implicit solvation effect was also considered using a ε = 2.1 isoelectric value which simulates the polarity of the mineral oil [48]. The calculations were performed using the VASPsol[49, 50] add-in package.

Results and discussions

Experimental Inhibition

Table 1 Results obtained for BTAH, 5-amine-BTAH and 5-methyl-BTAH in the inhibition assays at 200 ppm DBDS in dielectric oil.

		Benzotriazole concentrations		
Compound	DBDS (ppm)	2 ppm	3 ppm	4 ppm
BTAH	200	inhibition	inhibition	inhibition
5-amine-BTAH	200	corrosion	corrosion	corrosion
5-methyl-BTAH	200	inhibition	inhibition	Inhibition

Table 1 summarizes the inhibition assay results obtained for BTAH, 5-amine-BTAH and 5-methyl-BTAH when tested in dielectric oil at 200 ppm DBDS in a range of concentrations varying from 2 to 4 ppm of substituted-BTAH. For the 5-amine-BTAH, corrosion was obtained at all concentrations tested, after 72 hours. In contrast, for the same period, 5-methyl-BTAH and BTAH showed inhibitory capabilities in the entire range of concentrations tested.

Geometric and Energetic Aspects

The distances (d) between the adsorbate and the surface d(N-Cu) and between the nitrogen atoms of benzotriazole d(N-N) for the most stables complexes obtained in the study are reported in **Table 2**. In the complex formed with radical form of benzotriazoles, the adsorbate is closer to the surface than in the case of the molecular species, which is in agreement with the known higher reactivity of radicals. The triazole N-N distances in the complexes formed with radical structures are slightly larger than those obtained with molecular 5-substituted benzotriazol complexes.

The most stable adsorption complexes obtained after interaction via the nitrogen atoms of BTA● (or BTAH) on the possible Cu(111) surface adsorption sites (top, hollow hcp, hollow fcc, and bridge) are shown in the **Figure 2**.

Table 2. Selected N-Cu and N-N distances (in Å) for the most stable *BTA(H)*-Cu(111) adsorption complexes obtained using the PBE approximation.

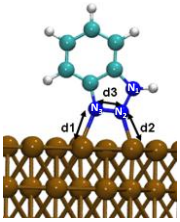

COMPLEX	d1	d2	d3
BTA● ··· Cu(111)	1.99	1.98	1.37
5-Amine-BTA●···Cu(111)	1.99	1.97	1.38
5-Methyl-BTA●··· Cu(111)	1.98	1.99	1.37
1-Amine-BTA···Cu(111)	2.12	2.27	1.36
1-Methyl-BTA···Cu(111)	2.17	2.13	1.31
BTAH···Cu(111)	2.25	2.21	1.32
5-Amine-BTAH ···Cu(111)	2.22	2.16	1.32
5-Methyl-BTAH ··· Cu(111)	2.34	2.49	1.30

The main adsorption site for two nitrogen atoms of the BTA(H) species in contact with the Cu(111) surface is a top-bridge-top site, while the other adsorption sites yield complexes with higher energy i.e. less stable (results not shown). This trend is found to be independent of the phenyl tilt angle between BTA and the surface. The perpendicular orientation found in this work is in agreement with those found in the literature, where the interactions over top sites and the angle of adsorption over the surface were described[20, 51]. These results will be used to characterize the other structures obtained.

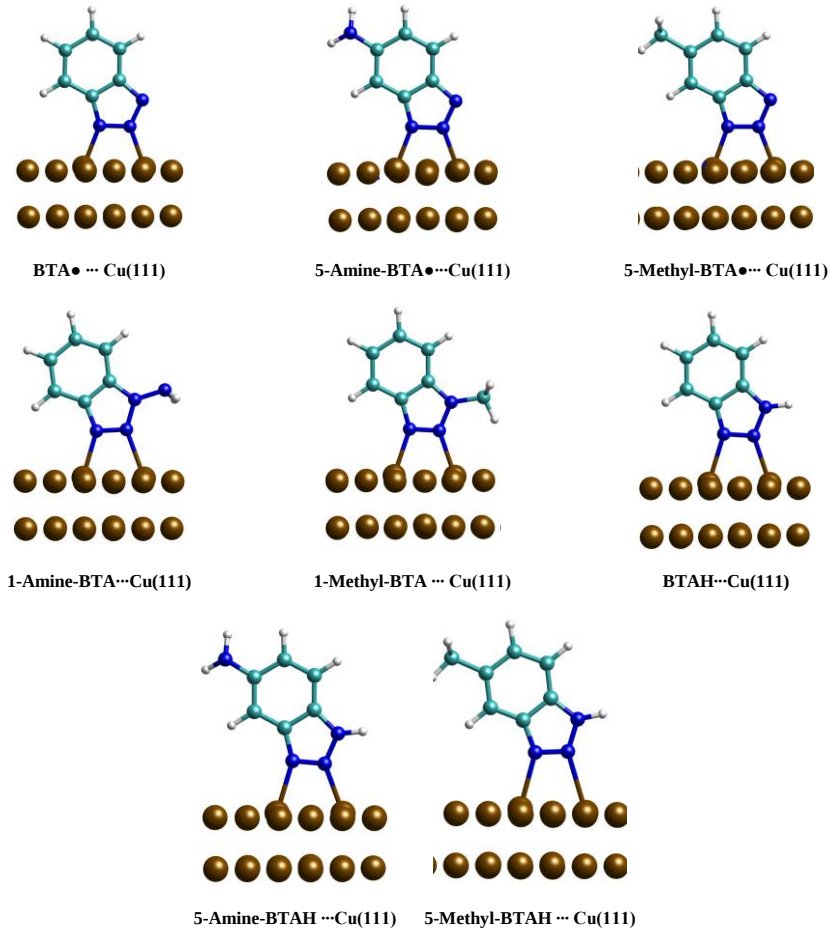

Figure 2. The most stable *BTA(H)*-Cu(111) complexes obtained using the PBE method. In the ball-and-stick representation, carbon, nitrogen, hydrogen and copper atoms are colored in green, blue, white and brown respectively

In general, the most favorable adsorption site was found to be the bi-coordinated top site. The perpendicular orientation adsorption was preferred instead of the parallel one. In the case of BTAH and its derivative compounds, the adsorption energies were lower compared with BTA● and could be classified as physisorption process in contrast with the chemisorption processes for the radical forms.

Table 3 shows the adsorption energies for the most stable complexes obtained, which are in agreement with the distance between adsorbate and surface, described previously. Comparing the adsorption energies of all BTAH and BTA● based structures, it is clear that the absence of a hydrogen atom in position N1 (BTA●), favors the adsorption on the Cu surface and the presence of a substituent in that position (N1) decreases the adsorption energy.

From a thermodynamic point of view, the most stable complexes (higher adsorption energies) correspond to those with small deformation of adsorbate and the highest interaction energy between deformed moieties. The copper surface remains almost unaltered in the adsorption process. The complexes formed with BTA● and 5-methyl-BTA● have similar and higher adsorption energies than 5-amine-BTA●, which is in agreement with the experimental results of copper corrosion inhibition (**Table 1**). Then, the higher the adsorption energy the higher the inhibition capacity will be. The same energetic trend was found in all cases studied with or without inclusion of the solvent effect.

The complex stability trend, mainly with radical forms, being in agreement with the adsorption energies (best inhibitory capacity), can be summarized as follows:

BTA● ≈ 5-methyl-BTA●> 5-amine-BTA● >> 1-amine-BTA > 1-methyl-BTA > 5-amine-BTAH ≈ 5-methyl-BTAH ≈ BTAH

Table 3. Adsorption energies (ΔE_{ads}) under vacuum and solvent conditions ($\Delta E_{adsSOLV}$) for the most stable complexes of *BTA(H)* derivatives. Energies in eV.

COMPLEX	**ΔE_{ads} PBE**		**ΔE_{def} PBE**		**ΔE_{int} PBE**
	Gas	SOLV	Cu	BTA(H)	
BTA● ··· Cu(111)	-2.86	-2.80	0.15	0.04	-3.05
5-amine-BTA●···Cu(111)	-2.36	-2.25	0.15	0.29	-2.80
5-methyl-BTA●···Cu(111)	-2.71	-2.69	0.15	0.17	-3.03
1-amine-BTA···Cu(111)	-0.72	-0.76	0.12	0.22	-0.85
1-methyl-BTA···Cu(111)	-0.55	-0.49	0.05	0.06	-0.55
BTAH···Cu(111)	-0.32	-0.40	0.19	0.04	-0.32
5-amine-BTAH···Cu(111)	-0.48	-0.57	0.15	0.02	-0.48
5-methyl-BTAH···Cu(111)	-0.36	-0.45	0.09	0.01	-0.36
DBDS···Cu(111)[1]	-1.67**	-			

***Adsorption Energy obtained using geometries from reference [32].*

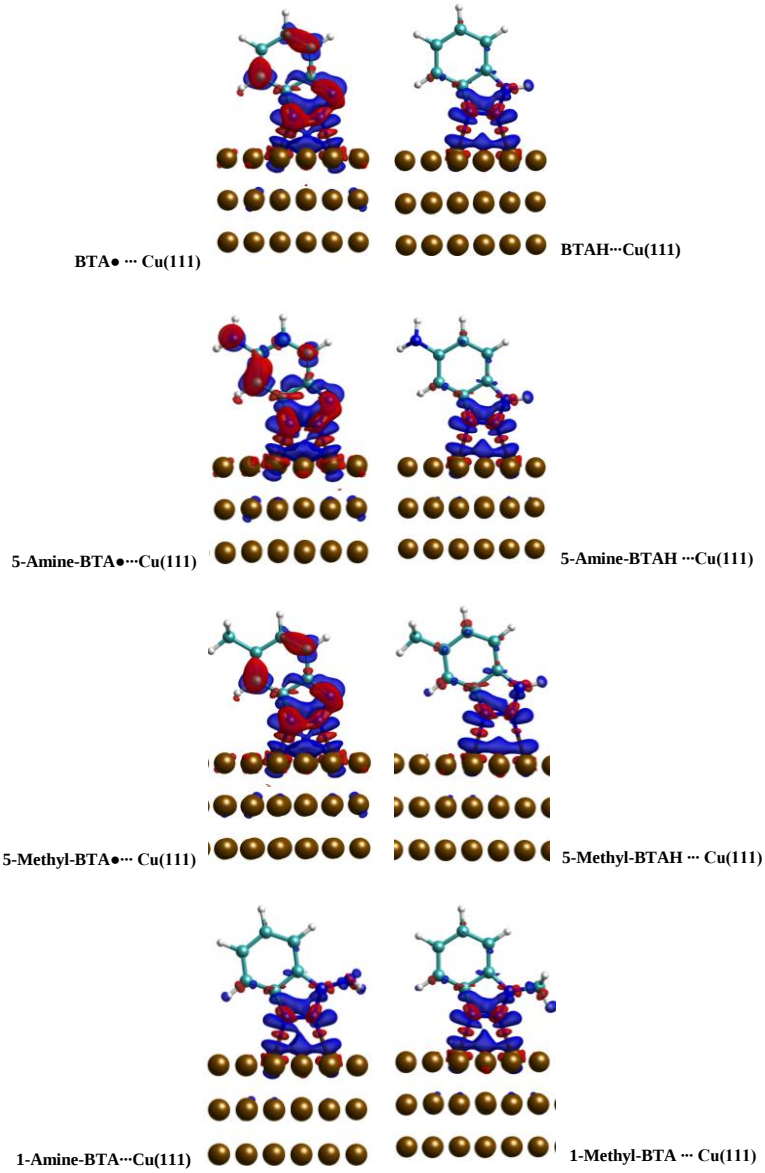

Figure 3. Charge density difference for the most stable *BTA(H)*-Cu(111) complexes. The blue (red) color represents the electron deficit (excess) regions, i.e., charge flows from blue to red regions.

Electronic Aspects

Global Charge Transfer

A global charge transfer descriptor was introduced to quantify the relation between the adsorption energies and charge transfer between adsorbate and surface. **Table 4** summarizes these quantities

considering the Bader and DDEC6 methods. In the first one, a charge transfer was observed essentially on the complex formed with radical structures of the adsorbate which is not present in the cases of molecular BTAH derivatives. It can be noticed that the direction of the charge transfer is mostly given from the surface to the benzotriazoles, where the azole group in the interaction with Cu surface acts as an electron acceptor moiety. Clearly, the transferred charge is allocated on the azole group and the surface (see **Figure 3**), reaching a maximum when a higher N-Cu interaction is obtained.

The charge difference, Δq, is reported in the last two columns of **Table 4**. It was calculated as the difference between the charge of the corresponding nitrogen atoms in the Cu(111)-adsorbate system, and the charge on the same atoms in the isolated adsorbate. About 70 % of the charge transferred is located on nitrogen atoms (N_2 and N_3) in contact with the surface and between 10-15% over the other nitrogen atom,

Table 4. Charge transfer (CT), Charge difference Δq, over N_2+N_3 and N_1+N_2+N_3 atoms under vacuum for the most stable complexes obtained.

COMPLEX	**CT ($q_{adsorbate}$)**		**Δq (N2+N3)**	**Δq (N1+N2+N3)**
	Bader	DDEC6		
BTA● ··· Cu(111)	-0.59	-0.16	-0.42	-0.48
5-amine-BTA●···Cu(111)	-0.52	-0.13	-0.39	-0.32
5-methyl-BTA●···Cu(111)	-0.55	-0.15	-0.52	-0.45
1-amine-BTA···Cu(111)	0.07	0.34	-0.20	-0.18
1-methyl-BTA···Cu(111)	-0.01	0.36	-0.15	-0.09
BTAH···Cu(111)	0.08	0.34	-0.07	-0.03
5-amine-BTAH···Cu(111)	0.10	0.38	-0.12	-0.11
5-methyl-BTAH···Cu(111)	0.08	0.28	-0.08	-0.11
DBDS···Cu(111)[1]	-0.76			

The complexes with the higher adsorption energies correspond to complexes formed by higher charge transfer from the surface. No significant effect was appreciated when a substituent was included at position 5 of benzotriazole, the charge transfer (CT) remains unaltered, in both cases, with the complex formed by radical or molecular forms. In the complex formed with the benzotriazol N_1 substituted, the charge transfer decreases and a lower stability was obtained. Using DDEC6 atomic population analysis, the CT values change but the electronic description is similar, a charge transfer from surface to adsorbate is appreciated for the most stable complexes and charge transfer in the opposite direction characterized the lowest ones.

The same charge transfer process can be analyzed through the charge density difference, $\Delta\rho(r) = \rho_{BTA(H).Cu(111)}(r) - \rho_{BTA(H))}(r) - \rho_{Cu(111)}(r)$ (See Figure 3.). In this figure, electron charge accumulation regions are shown in red whilst those with deficit are blue. The formation of nitrogen metal interaction is clearly seen by the charge redistribution between the corresponding nitrogen and the surface. The charge flows from the copper atoms of the surface (blue region) to the region between the nitrogen and the metal atoms (red region). The charge density difference pattern clearly shows different electron redistributions for the radical and molecular form of the analyzed benzotriazoles. In general, higher red charge accumulation regions located in the middle of the N-Cu interaction region and larger charge electron redistribution (including phenyl ring) characterize higher adsorption energies. The electron redistribution is a consequence of the resonance structures over both rings in the dehydrogenated species. Interesting to note is that when the N1 position is occupied by a substituent this is not the case. Although, a substitution in position 5 decreases the adsorption energy in dehydrogenated benzotriazoles, the inductive effect of the methyl group does not destabilize the electronic redistribution in such extend as does the amine group. Consequently, a stronger adsorption is obtained for the BTA●···Cu(111) and 5-Methyl-BTA●···Cu(111) complexes, than for 5-Amine-BTA●···Cu(111).

Comparison between benzotriazoles and DBDS adsorptions.

The present study considers a new perspective on the inhibition of copper corrosion process produced by *DBDS*. In earlier studies, the adsorption of *DBDS* over a Cu(111) surface was

characterized, and disulfide bond dissociation was observed in the complexes obtained by the chemisorption mechanism[32,33]. It was linked to the charge transfer processes in which higher deformation energy of the adsorbate was observed. A comparison between the ΔE_{ads} of BTA● derivatives and *DBDS* at PBE level shows stronger interaction of BTA● derivatives than for DBDS, indicating that the complex formed with BTA● derivatives are more stable. Although, greater charge transfer was observed from surface to the DBDS (-0.76e$^-$), the accumulation over sulfur atoms produces a disulfide dissociative process. This is clearly seen when the charge density difference between DBDS and BTA● adsorbed on Cu surface (Figure 4) are compared, i.e. a higher accumulation between S-Cu interaction region can be observed. But globally, the interaction with DBDS produced high deformation of DBDS adsorbed leading to a lower adsorption energy.

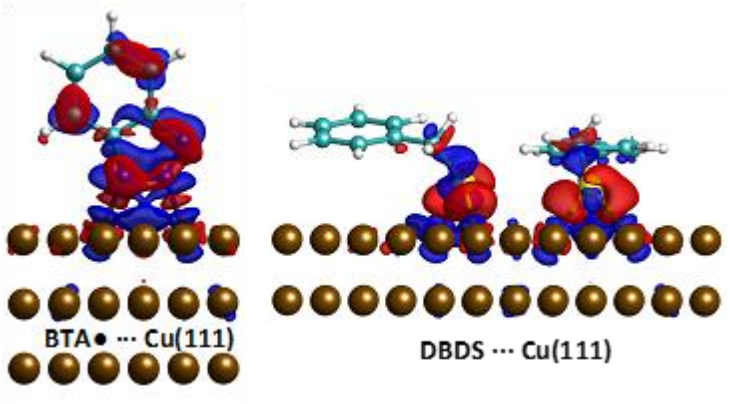

Figure 4. Charge density difference for *BTA*● and DBDS adsorbed on Cu(111) surface.

In both cases, the bi-coordinated interaction was found, but the orientation of the phenyl rings differs. A parallel orientation with the Cu surface was observed in the most stable DBDS-Cu surface complexes whilst a perpendicular adsorption was obtained for the benzotriazole and its derivatives.

Finally, in the case of molecular benzotriazole derivatives, the complexes have notably lower stability than those formed with *DBDS*, which infers a lower surface passivation for benzotriazole, i.e. the sulfur compound is more reactive than the nitrogen containing one.

Conclusions

The molecular adsorption of *BTAH* and selected derivatives on Cu(111) was characterized by periodic DFT methods. The adsorption was investigated considering energetic and electronic aspects over possible adsorption sites. The adsorption energies were calculated both in vacuum and including solvation contribution effects. A preferable adsorption site was found as a bi-coordinated atop site. The charge transfer between adsorbate and adsorbent was used to describe the electronic structure of the adsorption complexes. According to Bader population analysis, it was found that a charge transfer occurs from the surface Cu(111) to benzotriazoles, whereas in the processes with BTAH or molecular forms, the complex shows a lower, almost negligible, rate of charge transfer.

The radical species adsorb more strongly than their molecular counterpart. It was found that an amine group located in position 5 decreases the interaction energy by resonance effect, whereas a methyl group located in the same position increases the interaction energy by inductive effect. The role of benzotriazole as passivator was described and compared with *DBDS*. In both kinds of complexes formed, the electron transfer occurs from the surface to the adsorbate., The higher charge transfer to DBDS, activates the disulfide bond dissociation process. An larger geometrical deformation was found for DBDS , lowering its adsorption energy.

In contrast, including the passivator, the charge transfer is exclusively responsible for the adsorbate-surface interaction. A low deformation of adsorbed benzotriazol was determined which yields a higher adsorption energy than when the corrosive agent is adsorbed. In this way, our study rationalizes the corrosion/passivation phenomenon on the Cu(111) surface, using BTA derivates as passivator.

Acknowledgements

The authors acknowledge the financial support from FONDECYT through the Grant number 1120785 and to Universidad Andres Bello Grant DI-1322-16/R. M.S.-T. thanks to CONICYT for a Ph.D. scholarship. F.T. is grateful to FONDECYT and Universidad Andrés Bello for several appointments as Invited Professor. J.C.S. thanks to LABoratory of EXcellence Program: LABEX

Matisse for funding a research stay at Laboratoire de Chimie de la Matière Condensée de Paris of the UPMC.

REFERENCES

1. D. Chadwick and T. Hashemi, *Corrosion Science*, 1978, **18**, 39-51.
2. M. Finšgar and I. Milošev, *Corrosion Science*, 2010, **52**, 2737-2749.
3. D. Gallant, M. Pézolet and S. Simard, *Electrochimica Acta*, 2007, **52**, 4927-4941.
4. K. F. Khaled, *Electrochimica Acta*, 2009, **54**, 4345-4352.
5. K. F. Khaled, M. a. Amin and N. a. Al-Mobarak, *Journal of Applied Electrochemistry*, 2009, **40**, 601-613.
6. K. F. Khaled, S. A. Fadl-Allah and B. Hammouti, *Materials Chemistry and Physics*, 2009, **117**, 148-155.
7. A. Kokalj, S. Peljhan, M. Finšgar and I. Milošev, *J. Am. Chem. Soc.*, 2010, **132**, 16657-16668.
8. G. Laguzzi, L. Luvidi and G. Brunoro, *Corrosion Science*, 2001, **43**, 747-753.
9. A. K. Satpati and P. V. Ravindran, *Materials Chemistry and Physics*, 2008, **109**, 352-359.
10. S. T. Selvi, V. Raman and N. Rajendran, *Journal of applied electrochemistry*, 2003, **33**, 1175-1182.
11. A. Solehudin, *International Refereed Journal of Engineering and Science*, 2012, **1**, 21-26.
12. W. Stefan, a. Jutta Jakobs and T. Reemtsma, *Environ. Sci. Technol.*, 2006, **40**, 7193-7199.
13. L. Tommesani, G. Brunoro, A. Frignani, C. Monticelli and M. Dal Colle, *Corrosion Science*, 1997, **39**, 1221-1237.
14. R. Walker, *Corrosion*, 1975, **31**, 97-100.
15. R. Walker, *J. Chem. Educ.*, 1980, **57**, 789.
16. V. Brusic, M. Angelopoulos and T. Graham, *J. Electrochem. Soc.*, 1997, **144**, 436-442.
17. X. Chen and H. Häkkinen, *Journal of Physical Chemistry C*, 2012, **116**, 22346-22349.
18. Z. Chen, L. Huang, G. Zhang, Y. Qiu and X. Guo, *Corrosion Science*, 2012, **65**, 214-222.
19. C. Gattinoni and A. Michaelides, *Faraday Discuss.*, 2015, **180**, 439-458.
20. F. Grillo, D. W. Tee, S. M. Francis, H. Früchtl and N. V. Richardson, *Nanoscale*, 2013, **5**, 5269-5273.
21. A. Kokalj and S. Peljhan, *Langmuir : the ACS journal of surfaces and colloids*, 2010, **26**, 14582-14593.
22. F. Ahmed Khan, J. Sundara Rajan, M. Z. a. Ansari and S. Asra P, *2012 International Conference on Advances in Power Conversion and Energy Technologies (APCET)*, 2012, DOI: 10.1109/APCET.2012.6302039, 1-4.
23. A. M. Y. Jaber, N. A. Mehanna and A. M. Abulkibash, *Journal of Separation Science*, 2012, **35**, 750-757.
24. R. Lakshmi and T. Murthy, *International Journal of Engineering Research and Technology*, 2012, **1**, 1-8.
25. M. Martins and A. Gomes, *Electrical Insulation Magazine, IEEE*, 2010, **26**, 27-32.
26. N. Mehanna, A. Jaber, G. Oweimreen and A. Abulkibash, *IEEE Transactions on Dielectrics and Electrical Insulation*, 2014, **21**, 1095-1099.
27. J. M. Lukic, S. B. Milosavljevic and A. M. Orlovic, *Industrial & Engineering Chemistry Research*, 2010, **49**, 9600-9608.
28. T. Amimoto, N. Hosokawa, E. Nagao, J. Tanimura and S. Toyama, *IEEE Transactions on Dielectrics and Electrical Insulation*, 2009, **16**, 1489-1495.
29. S. Toyama, J. Tanimura, N. Yamada, E. Nagao and T. Amimoto, *IEEE Transactions on Dielectrics and Electrical Insulation*, 2009, **16**, 509-515.

30. R. Maina, V. Tumiatti, M. Pompili and R. Bartnikas, *IEEE Transactions on Dielectrics and Electrical Insulation*, 2009, **16**, 1655-1663.
31. D. Costa, C.-M. Pradier, F. Tielens and L. Savio, *Surface Science Reports*, 2015, **70**, 449-553.
32. M. Saavedra-Torres, F. Tielens and J. C. Santos, *Theoretical Chemistry Accounts*, 2015, **135**, 1-9.
33. M. Saavedra-Torres, P. Jaque, F. Tielens and J. C. Santos, *Theoretical Chemistry Accounts*, 2015, **134**, 1-9.
34. F. Tielens, V. Humblot and C.-M. Pradier, *Surface Science*, 2008, **602**, 1032-1039.
35. N. Kovačević and A. Kokalj, *Corrosion Science*, 2013, **73**, 7-17.
36. B. Hammer, L. B. Hansen and J. K. Norskov, *Physical Review B*, 1999, **59**, 7413-7421.
37. J. P. Perdew, K. Burke and M. Ernzerhof, *Physical Review Letters*, 1997, **78**, 1396-1396.
38. H. Rieley, G. K. Kendall, A. Chan, R. G. Jones, J. Lu¨decke, D. P. Woodruff and B. C. C. Cowie, *Surface Science*, 1997, **392**, 143-152.
39. a. Ferral, E. M. Patrito and P. Paredes-Olivera, *The journal of physical chemistry. B*, 2006, **110**, 17050-17062.
40. E. R. Crutcher, K. Warner and M. Northwest, *electric-connectionco.com*.
41. X.-L. Fan, Y. Liu, R.-X. Ran and W.-M. Lau, *The Journal of Physical Chemistry C*, 2013, **117**, 6587-6593.
42. M. E. Straumanis and L. S. Yu, *Acta Crystallographica Section A*, 1969, **25**, 676-682.
43. S. Grimme, *Journal of computational chemistry*, 2006, **27**, 1787-1799.
44. A. Tkatchenko and M. Scheffler, *Phys Rev Lett*, 2009, **102**, 073005.
45. J. Scaranto, G. Mallia and N. M. Harrison, *Computational Materials Science*, 2011, **50**, 2080-2086.
46. G. Henkelman, A. Arnaldsson and H. Jónsson, *Computational Materials Science*, 2006, **36**, 354-360.
47. W. Tang, E. Sanville and G. Henkelman, *Journal of physics. Condensed matter : an Institute of Physics journal*, 2009, **21**, 084204.
48. V. M. Shkol'nikov, L. A. Bronshtein, Y. N. Shekhter and O. L. Drozdova, *Chemistry and Technology of Fuels and Oils*, 1977, **13**, 479-481.
49. K. Mathew, R. Sundararaman, K. Letchworth-Weaver, T. A. Arias and R. G. Hennig, *The Journal of chemical physics*, 2014, **140**, 084106.
50. M. Fishman, H. L. Zhuang, K. Mathew, W. Dirschka and R. G. Hennig, *Physical Review B*, 2013, **87**.
51. F. Grillo, D. W. Tee, S. M. Francis, H. A. Früchtl and N. V. Richardson, *The Journal of Physical Chemistry C*, 2014, **118**, 8667-8675.